ISSN 1330-3651 (Print), ISSN 1848-6339 (Online)
https://doi.org/10.17559/TV-20240126001294
Original scientific paper

Edge Computing Assisted Internet of Things in Sports Management System

Baolei ZHANG, Juan YANG, Yan PENG, Chong LIU*

Abstract: In recent years, the movement analysis is commonly used to track the risk of injury and strengthen the efficiency of athlete performance. However, most of these devices are costly, found mainly in experimental settings, which analyze a few samples of each movement. In this paper, a new ambulatory movement analysis system with wearable sensors for the precise measurement of all athlete's movements in an actual training scenario is introduced. Initially, an adaptive method categorizes a broad variety of training behaviors by the Differential Finite element Transformation method (DFET) along with a Random Forest Classification (DFET- RF) method. Secondly, the measurement of the absolute identities of the wearable sensor devices placed on the knee bone and pelvic bone is performed with a discrete gradient descent (DGD) algorithm, which calculates a range of motion-extension between the knee and hip angle. Finally, the edge computing is used to process data in real-time and reduce the latency of the system. The next version of wearable technology will know the person's identity, individually - not just physically and actively in a much more significant way; a wearable device that tells the world about the identity of the person and the connected devices. The knee flexion is greater at the terminal swing period (85%) and hip flexion (68%). The development of future device capabilities is based on verification. Once a wearable can validate the wearer's identity, several other things about their activities can be regulated. Such angles are automatically extracted for each movement during jogging at the acceleration of the sacrum effect. Besides, standard data has developed and is used to decide whether the movement methodology for a person varied from the standard data to classify potential instances due to injury. This is done by a gradient-shift recording technique for the joint-related angle details. For precise and automated assessment of athletic movements, effective activity measurement in various uncontrolled conditions for both injuries processing performance progress, the suggested system has been discussed in this paper.

Keywords: discrete transformation; discrete gradient; edge computing; finite element; random forest classification

1 INTRODUCTION

Sports and physical exercises provide a major neurological, musculoskeletal, and psychiatric impact [1]. However, lower body muscular injuries are very normal [2]. About any damage attributed to the extreme severe tissue load results in heavy load in comparison to the intensity of the tissue. Movement methodology greatly affects this load [3, 4]. Athletes should be biomechanically tested to evaluate the predisposition for athlete's injury by measuring and quantifying both their joint position and radial velocity. Any indicator of loading on their organs during a sequence of acts specific to their activity is considered to be linked to injury [5, 6]. Typically, the participant performs 1-3 full commitment trials of each movement and their outcomes are linked to universal standards. Such experiments are mostly performed in laboratories as camera-driven solutions which will stay spatially stable throughout the training session but appear to be influenced by a shift in lighting conditions and prefer to be biomechanically dependent movements for analytics solutions [7]. This screening method poses multiple obstacles to determine and evaluate, which significantly reduces the environmental value and usefulness. The screening will diagnose the problem quickly. Detecting an obvious issue may lead to much more successful care. The barriers entail distinguishing previous or current musculoskeletal damages. Severe arthritis disabilities, especially with large muscle mass joint, include allergy, multisystem disease, and high-temperature disease symptoms.

It includes the participants who are very concentrated on how they execute the exercises and therefore cannot utilize a movement system which they typically might use for an exercise or match. The regulated experimental atmosphere is not modeled as the same for training conditions. It is quite controversial to use just 1 to 3 exercises as a way of demonstrating how well an athlete performs a movement strategy. Due to the considerable cycle time associated with optical systems, the small number of tests is normal. The small number of athletes evaluated is the consequence of a shortage of procedural evidence on certain sports-based activities. The far more important sports facts are health implications that avoid or mitigate issues with health and well-being. It saves burden on healthcare. Training effects can cause some health consequences, typically for teenagers, but in contrast, exercise has a greater, more economical, and more significant positive health impact on older adults. This is an expensive technology that limits the general usage [8, 9].

Sensors that can be used during a training session or sports event to track joint lateral activity and effect accelerations of athletes may be a solution to the above performance challenges [10]. Depending on Newton's second rule of motion at some ground touch, the accelerometers placed on the body may be used to predict load [11]. Microtechnology tracking in sport enables player location, speed, and muscle activation to measure. A navigation system offers a stronger knowledge of normal metabolic and functional challenges. It could be used to improve workout routines that equip participants properly for success in optimizing on-the-spot results.

Every foot will touch the ground more than 1500 times in a 30-minute workout. Taking advantage of microtechnology in sports or natural conditions, the cost-effective, miniaturized, low-mass and non-invasive instruments may have been created to track the movement, and near-real-time responses of individuals. In contrast with optical and visual devices, these latest solutions are accurate enough to resolve the issues. Like accelerometers and gyroscopes, object tracking sensors are excellent examples of MEMS devices, which utilize the micro-technology to track, identify and calculate different human activities [12]. Wearable measurement tools can track rotational and translational motions, which gain prominence in a range of athletic activities, recovery, and everyday practices to control human motions [13-15]. This allows a patient to track and then modify his or her behavior outside of the therapeutic setting continuously. In conjunction with an enhanced algorithm to assess sensor orientation in better detail, it has been possible to deploy wearable body sensor networks in training sessions with the latest creation of a more specific and comparatively cheaper device [16, 17]. It categorizes rising foot-ground touch instantly and reliably, depending on the movement style of the individual, such as walking, jogging, sprinting, running, floor, strength split, etc., [18, 19]. The growing demand for mobile devices has resulted in the growth in service requests from mobile devices to edge servers, requiring the reform and innovation of traditional cloud computing. Mobile edge computing technology focuses on the customer, reducing response times and increasing service experience. Low latency has been improved in the CSMA/CA (Carrier Sense Multiple Access with Collision Avoidance) handshake method and MAC layer architecture. The A priori algorithm is used to improve athlete training data and generate individualized workout plans [20]. A program of this type is currently not accessible to the full understanding of the writer. While there are few studies, evaluating data poses a variety of challenges.

- Prolonged data are usually limited to a single discrete step, ostensibly a joint activity scientific. In fact, less than 1% of the available data is included [21].
- Continuous data includes differences in phase and amplitude between people and in many trials per person [22].

Standard data is usually produced each time where the experiment is normalized to 100 data points and summed in each of the studies. Therefore, this might skew the results, because the main activity is not limited over time between trials.

Such issues can be solved with successive empirical results; few biomechanical experiments have been tried. The purpose of this analysis is to use wearable sensor devices [23, 24]:

1. Formulate each ground touch according to the style of movement automatically and reliably.
2. Automatically extract data for each foot connection phase from the joint angle and impact torque.
3. Generate normal data for joint angle data utilizing an approach to practical data, for result acceleration data with a distinct data point.
4. Compare a person to the procedural data and describe the different phases.

This paper is an expansion of prior experimental research. This research is broadened by analyzing the hip joint inclination and the direction of the sacral effect for evaluating and referencing various forms of classification.

2 MATERIALS AND METHODS

The core components of our system, as shown in Fig. 1, include: the description of movement, the definition and measurement of the peak impact acceleration of sensor and knee- and hip angles of flexion expansion and the study of technology. The accelerations of sacrum effect, and the angle of bone and hip bone flexion to demonstrate the mechanism helps to prevent unintentional redundancy in this article.

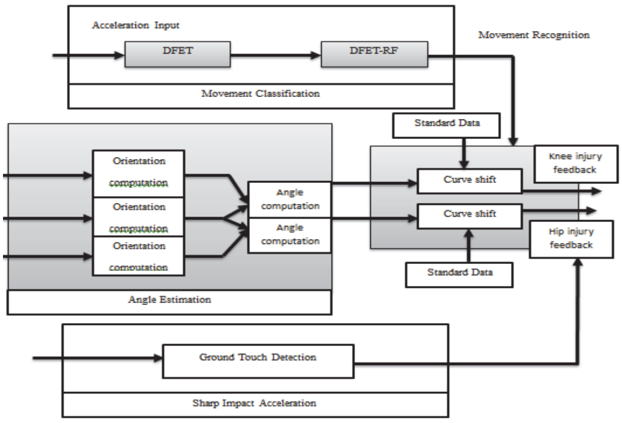

Figure 1 Schematic of the proposed system

2.1 Participants

For the intent of testing the suggested system, six wearable sensors have been used to monitor the behavior of 10 stable individuals and one disabled with spinal pain. Subjects with varying degrees of knowledge experience have been selected to explore the system in several ways. On the two orientations leg, and the pelvic bone and tailbone of an individual have been positioned wearable sensor units. The positioning of the wearable sensor on each body part has been used to prevent broad masses of muscles, as weaker tissue deformities will adversely affect the acceleration of impact and the precision of the joint orientation calculations due to contraction of muscle and ground touch results. In sports, weaker tissue deformities are among the most frequent criticisms, occurring in both players and non-athletes. These tissue deformities constitute a challenge for experts in the face of a sluggish rehabilitation that prevents athletes from practice and competition. Many of these injuries are caused by excessive stretching or direct muscle belly trauma. In evaluating potential damages, the biomechanics of the wound must be considered; further, the mobility and output of the subject, where the wearable sensors have been connected to the individual with a stripe on certain cloth elasticity. Next, the issue has been challenged to take a course of action during the outdoor workouts. On a large grass soccer field, each athlete followed a predefined training regimen. The workout schedule included: fitness breaking, cycling, sprints, jogging, box running, and free kicks in soccer. For the whole session, the average length of each motion has been about 1 minute for around 9-10 minutes. Every sensor data has been collected on the computer by an existing Memory card. Because each sensor registered data separately, both sensors needed to be synchronized by a physical cause. Grouping the operation and training given to the team of players as segments will be more beneficial. Every player learns from each other and encourages each other to resolve barriers of sports practice together. Experiencing community success and failure would foster morality, camaraderie, and better coordination. The directions have been provided for 5 vertical jumps for each subject, ensuring significant acceleration spikes have been simultaneously seen in each unit visible in the accelerometer stream. The peak alignment has been automatically performed in a post-processing stage and all information streams have split in 3 seconds before the first high jump landing.

2.2 Movement Classification

The automated grouping of operations is used to classify specific training practices so training exercises can be judged by sports practitioners and healthcare professionals more easily. This will enable them to segment a training session by operation rapidly and thus to conveniently find the required data. That method allows it possible to build a database that includes the recording of the actions of an individual during training sessions. Edge computing is important in sports movement analysis because of its ability to process data in real-time near its source, reducing latency. This method consumes less bandwidth, improves privacy and security, and is scalable for large-scale events. Edge computing is adaptable to environments with limited connectivity, potentially saving money by reducing reliance on cloud services. It also enables customization and specialized processing, allowing analyses to personalize to specific sports or team requirements. In summary, edge computing improves sports decision-making through fast, efficient, and secure data processing.

For this work, the most reliable classification scheme has been tested by four separate classifiers, LBK, RBF Network, NB and RF classifications. The LBK type is k-NN. k-NN has proved to be effective in problems with human behavior. An RBF Network classifier system has been very effective in distinguishing between various human activities. NB is a Bayesian classifier used in several classification problems. Many recent studies in movement classes have been associated with the recognition of repetitive behaviors such as taking food, up and downstairs, and performing movements, such as standing, walking, jogging, and sports workouts. New work has been found that human behavior can be graded with accelerometers for energy-intensively sprinting, jogging, leaping and more. For athletics, professional athletes in athletic and fitness conditions have been tracked using the accelerometer. For the retrieval of intra- and inter-stroke stages, they are used to test techniques during active rowing. Accelerometers have been often used to classify many steps of the chain during sporting service.

The preparation practice conducted by each athlete has been the first section and annotated for all tasks in designing our approach to classification. A 3-second period has been used to complete every picked exercise. DFET has been effectively used to remove biased characteristics of the used accelerometer data as a framework for further classification. Accelerometers are motion monitoring systems capable of capturing the physical activity rate. They usually stick to an individual's tail with a belt loop, but some monitors may be working on the handle, ankle, or shoe. The wavelet converts the function by breaking down a signal in many iterations of a chosen mother wavelet which are transferred and sized. Such PQR dimensions have been used to classify football and field hockey sports events. D wavelet, because of its regularity and quick computational time, is the common option for the mother wavelet in signal analytics chosen. To increase the frequency resolution further, the output coefficients provided by the DFET may be decomposed. The degree a is increased with every additional decomposition. At level a of the DFET decomposition, the total energy E_s is provided by Eq. (1).

$$E_s = I_a I_a^T + \sum_{b=1}^{a} J_b J_b^T \tag{1}$$

where, I_a is level a, I_a^T is the transposition of I_a and J_b is the vector of approximation at level a. The energy ratio for each form of the coefficient is a function that has proven useful in discrimination. EDR_i represents the approximation coefficients energy ratio, while EDR_b represents the accurate data energy ratio.

$$EDR_i = \frac{I_a I_a^T}{E_T} \tag{2}$$

$$EDR_b = \frac{J_b J_b^T}{E_T} \tag{3}$$

The most insightful features for a separate issue have been the standardized variances of the DFET decay coefficients and the EDR. In comparison with their results, they obtained high success against knowledge such as uniform methods, EDR Minimums, and Maximums.

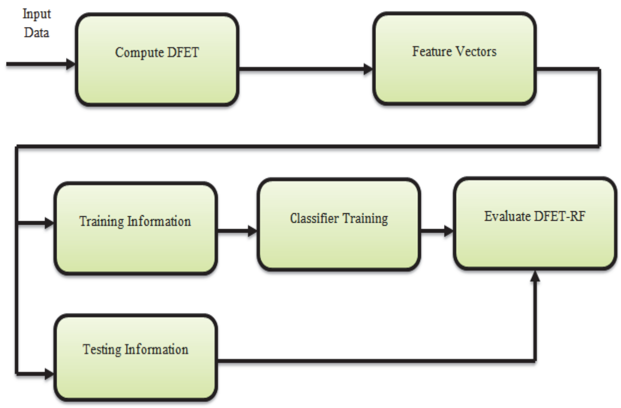

Figure 2 The Computation of DFET- RF

Here, the coefficient variances are measured at the i-th stage over the increasing DFET coefficient matrix. The development of an appropriate classification algorithm has been used with the DFET functionality as in Fig. 2.

3 THE ORIENTATION OF SENSORS AND MEASUREMENT OF JOINT ANGLES

Accurate instruction is an integral aspect of athletic practices because trainers, bio mechanists and athletic scientists will monitor and research the activity techniques of athlete's indoor and outdoor conditions. Although various systems exist for monitoring the methodology and body orientation of athletes, wearable inertial sensors gain from being autonomous of the action, the atmosphere, and position of the measurements. It is possible to determine orientation by three-axis gyroscopes and a filter in three-dimensional areas.

The algorithm adopts an orientation Cartesian coordinates representation. In the following Eq. (4), the projected orientation rate is specified.

$$\{U_{E^{CCT}} = U_{E^{CCT-1}} + U_{E^{CCT}} \Delta T\, U_{E^{CCT}} = U_{E^{cc\delta,t}} - \gamma \frac{\nabla g}{\|\nabla g\|} \tag{4}$$

where,

$$\{\nabla g, E^U, E_{f,}, U_i = B^{T(}E_{f,}, U_i) g\left(\nabla g, E^U, E_{f,}, U_i\right) 0 U_i = \\ = \left(0, i_x . i_y . i_z\right) E_f == \left(0,0,0,1\right) \tag{5}$$

Through such a configuration $U_{E^{CCT}}$ and $U_{E^{CCT-1}}$, the Surface of the groundstructure is aligned to the t and t – 1 dimensional sensor array. $U_{E^{CCT}} \Delta T$ is the intensity at which sensors calculate their shift in orientation. S_a is the x, y and z component, respectively, of the sensors, which are $\nabla g, E^U, E_{f,}, U_i$. By integrating the predicted orientation shift rate calculated with a sensor, the algorithm measures orientation $U_i = \left(0, i_x . i_y . i_z\right)$.

Then the sensor calculation error β centered on other sensor measurements, has been eliminated in a range. This method incorporates a strategy of DGD optimization to calculate one answer for the sensor orientation by understanding the position of the ground touch gravity. The decrease in the Centre of gravity improves athletic strength and control. It seems the legs bending and lowering to the surface will change their directions quicker. It enhances your flexibility so you can adapt the legs to more strength.

Here f is the target function and J is Jacobean and the following Eqs. (6) and (7) are described.

$$g\left(CC_T, U_i\right) = \\ \left[2(CC_{T4}CC_{T2}) - i_x\; 2(CC_{T1}CC_{T2}) - i_y\; 2(CC_{T3}CC_{T2}) - i_z\right] \tag{6}$$

$$J\left(CC_T\right) = \\ \left[2CC_{T1}\; 2CC_{T2}\; 2CC_{Te}\; 2CC_{T2}\; 2CC_{T3}\; 2CC_{T4}\; 0\; 2CC_{T4}\; 0\right] \tag{7}$$

The orientation output of the sensor is typically quantified as Root Mean Square errors. The standardized and Root Mean Square values are 0.543, and 0.421, respectively. Pitch and roll orientation components utilize the methodology defined. The 5RMS dynamic values of the orientation pitch and roll variable are 0.658 and 0.597 pcs. The algorithm, therefore, achieves precision levels that equal the algorithm.

A joint revolution is generally characterized as the anterior segment inclination towards the ventral segment. The two wearable sensors mounted to the anterior and the ventral segments have been measured by the calculation of the flexion-extension joint angles. A practical configuration has been defined for aligning the frame of each sensor device to the body structure. A defined technique for calculated knee joint angle flexion-extension and measuring hip flexion-extension angle has been implemented in the shank and thigh parts and pelvis segments. The following Eq. (8) explains this:

$$\{CCT_{\text{joint}} = U_{E^{\text{high}}} \times U_{E^{\text{low}}}\, CCT_{\text{angle}} = U_{E^{\text{high}}} \times U_{E^{low}} \tag{8}$$

where, CCT_{joint}, CCT_{angle} reflect the pelvic, thigh position, respectively. The × denotes the result of matrix multiplication. Throughout the whole workout session, knee and hip joint ratios have been calculated.

4 ANALYSIS OF THE APPLIED TECHNIQUE

The task of this segment is the work of jogging. The selection has been created as it involves three events that would usually involve: an effect, where a loading process and a movement step have been calculated. The jogging activity has been focused on the details given by the above classification system. Cycles of foothold touch have been associated with knee joints and acceleration of the lower leg. Foot strike has been described as the sudden acceleration shift in knee articulation data after increasing the local cyclic maximum. Knee and hip articulated angles have eventually developed. Specific period profiles have been predicted to reveal identical variations in the knee and hip joint angle curves between trials and athletes. The standard curve has been generated by two methods to preserve all the details about the curve shapes: a visualization of the touch period without registering, which is the most common method in biomechanics, and the recording of the phase change until the foot touch process has been summed accordingly as in the Eqs. (9), (10) and (11).

$$i_a^*\left(t\right) = i_a(t + \mu_a) \tag{9}$$

$$SNE = \sum_{a=1}^{N} \int_0^T ([i_a\left(t + \mu_a\right) - \mu\left(t\right)]^2 \,\mathrm{d}t \tag{10}$$

$$SNE = \sum_{a=1}^{N} \int_0^T ([i_a^*\left(t + \mu_a\right) - \mu\left(t\right)]^2 \,\mathrm{d}t \tag{11}$$

The phase switch registration shifts the temporal domain by μ_a for each signal, a for certain μ_a to classify $T_j\, \mu_b$ if the identification conditions exceed the minimum for each signal.

The criterion used *SNE* (Squared Normalized Error) has been computed for each of the inputs relative to the total mean $\mu\left(t\right)$ (over its elapsed time t) and applied for each foot contact cycle to identify the optimal μ_a for each foot contact cycle a. The following are recorded by the optimal b. This transformation process is often referred to as the Procrustean method by converting it into an iteratively updated average. The curves have been analyzed using the Characterizing Phase Analysis to see whether there are variations between the average curve and a historical average curve. This method offers a more detailed contrast than a single analysis or practical key analysis of the item since it describes variance phases of the data used to produce the entity scores subsequently. A single analysis is a qualitative analysis that depends heavily on the analytical and integrative ability of the social context in which the information is collected. A practical key analysis examination is based on an ethically informed and participatory-in-context attitude and a collection of analytical methods is necessary to create and investigate.

A patient with joint pain has been tested to analyze the capacity of the new method to classify individuals with irregular movement physiology. Visually and clinically, variations have been investigated. By comparing confidence intervals boundaries of a single athlete with the 90% confidence intervals of the regular community results, a statistic discrepancy has been established. If the confidence ranges did not converge, harmonic frequencies have been found statistically distinct.

4.1 Numerical Validation Based on DFET-Forest Classification

Tab. 1 indicates how long various classification models need to train and evaluate. In test cases of results, each classifier has been analyzed based on the Multilayer Perceptron to train a single model approximately 15 minutes. The contrast of various classification criteria produces major congestion. The DFET- Random Forest has made almost instant data classification which in real-world scenarios is extremely desirable, as shown in Tab. 1

Table 1 Duration for testing and training

Classifiers	RBF	NB	LBK
Training Duration / sec	0.18	0.08	0.23
Testing Duration / sec	0.28	0.24	0.16

As shown in Tab. 1, overall, the most reliable has been analyzed by the DFET- random forest description. Walking is an incredibly low energy task and therefore any classifier can distinguish between it and other behaviors. Likewise, endurance has been analyzed based on the classifiers as requiring somewhat specific action styles and pace during a high-intensity exercise such as sprinting and kick-off. Endurance indicates that the cardiac output is more than 50 percent the limit and can do any activity. It can even be split into general stamina and particular stamina in the higher rank. The ability to cope with fatigue in such sport conditions is stamina, and General stamina characterizes the entire body's capacity to withstand and decrease exhaustion. Every operation has specific features to distinguish between each classifier. The DFET capacity, a limited number of features has been applied to each classification so that the classification phase has been quite simple.

Table 2 Parametric validation of DFET-RF during training

Movements	Accuracy / %	Recall	F-measurement
Walking	0.89	0.9251	0.971
Jogging	0.92	0.825	0963
Cycling	0.91	1	0.963
Long jumping	0.82	0.913	0.954
stretching	0.72	1	0.941

From the investigation, the DFET-RF reached the highest reliability within permissible algorithmic limits. Classification accuracy of 91.5% is obtained by the DFET-RF classifier. This value has been determined during the cross-validation process. The F-measurement score has been determined as a harmonic method of precision and reminder, which achieves the best 1 and 0 in the worst result. Accuracy Rate is calculated by dividing the correct results into the total results. Thus, an alert is divided by the number of positive results. Such measures are often defined as true positive and false negative measures. The F-measurement scores are given in Tab. 2, because the classification method is trained in groups of specific instance populations. The F-measure value indicates a model that can accurately classify an incident rather than the normal classified accuracy alone.

Table 3 Matrix representation for the DFET- RF

Movements	A	b	C	D	E
Walking	180	0	0	0	0
Jogging	0	242	0	0	0
Cycling	0	0	38	0	0
Long jumping	0	0	0	107	0
stretching	4	7	2	1	54

Tab. 3 presents the designation process uncertainty chart. This concept is kick-started by football just in one area of uncertainty. This is hardly attributable to the difference in kicking styles between men. F-measures range from 0.872 to 0.892 as seen in Tab. 3. The strongest F steps are walking and endurance split, followed by jogging, cycling, and soccer punches.

4.2 Technique Validation Based on Graphical Analysis

The participants have been required to jog for a minute during the virtual training experiment, with about 33-foot touch intervals for each participant. The created knee bone angle curves as shown in Figs. 3a and b have the typical form, with a narrow (0-31%) and wide (31-93%) flexion-extension chain. The mathematical study of the angle curve of the knee showed that the unrecorded and the reported medium curves vary greatly. The unregistered average curve revealed a considerably larger (p = 0,001) and lower value ($p < 0.002$), a larger (96%) and a smaller (60%-80%). The traditional extension series of 0-80 in the % location and at the early stages of the swing accompanied by a narrower extension bending period in the later stages (75-90 %) in the hip angles.

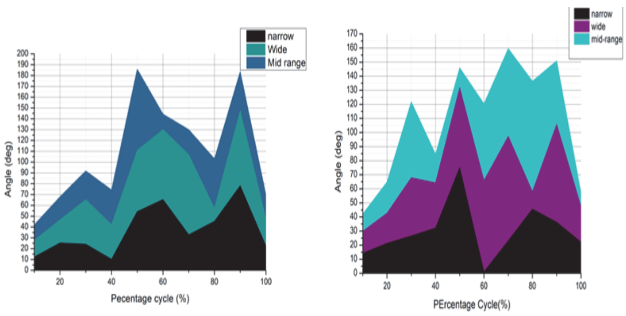

Figure 3 (a) Flexion cure for healthy subject; (b) Flexion cure for injured subject

Even the statistical study revealed substantial variations between the unrecorded and reported medium curves in the hip angle curves. For (15-25 %) and (75-85 %) of the foot touch period, the unregistered mean curve has been slightly smaller ($p < 0.01$) in magnitude. Differences in both the knee bone and the hip bone joints are evident at the inner individual stage. The recorded and non-reported curves are quite close except magnitudes between (15-30%) during the first step (1-50%) of the analyzed foot touch period. Yet all mean curves continue to exhibit variations in size, plan characteristics and standard deviation for phases above 50%. In the hip joint the recorded and unregistered curves exhibit similarity in certain stages as with the knee joint, but vary distinctly in the pre- and post-state periods.

The size and position of the peak hip bending clearly show the effect of the variability within the subject of the activity cycle, which causes an effect in the average curve. By comparing the ground touch cycles, an intra- or inter-subject variation affects the average produced curve and may lose very useful details on that topic. For injury trials that show a predisposition to the injuries or early stages of injuries that may need an appropriately qualified operation that may be particularly relevant for minor variations in typically safe individuals or changes over time as shown in Figs. 4a and b. The complicated data obtained is more important, especially if its derivatives are examined.

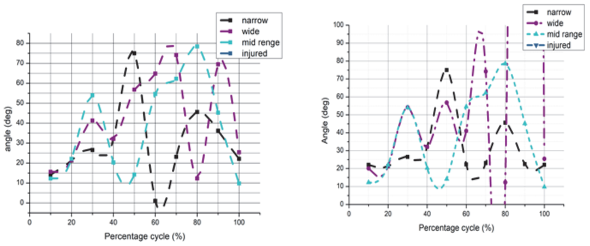

Figure 4 (a) Average knee angle - 1 injured individual; (b) Average hip angle - 1 injured individual

The knee usually bends at beginning load (0-12.0%) and early middle (20-35%) in normal subjects, whilst it stretches distinctly in the wounded person. The original load response is attributed to the biarticular muscle hamstring working concentratedly to stretch the hip and hold the spine upright, Fig. 4b, and results in knee folding as a function of the hamstring. The irregular knee bone stretch in the affected individual thus implies either an acceptable or injurious motion technique that shows that the trunk bends inappropriately during the initial loading reaction. This can be accompanied by higher hip and post heel bending angles. From a compensatory standpoint, this might be a technique to minimize the loading of lower back effects by eccentric trunk expansion systems. Maybe the knee bending is started a lot more sooner in an injured subject than usual in reaction to the irregular early knee extension. The greater knee flexion at the terminal swing period (85%) and hip flexion (68%) will suggest a running style to minimize stress loads and thereby decrease backpressure and further injury.

Our injured runner did not, though, improve his knee flexion at an early stage of the course, in comparison to prior records. Sacred peak impact accelerations have been immediately collected in 50 frames (0.14 sec) after the initial interaction with the ground by determining the small magnitude. The intensity of the sacral effect has been comparable to previous values recorded as in Fig. 5. There is little disparity between the ideals of disabled players and the Uninjured. As the force of such impacts is backbone axial stress, an athletic injury may mean vertebrae regulation instead of vertebrae supports or vertebrates.

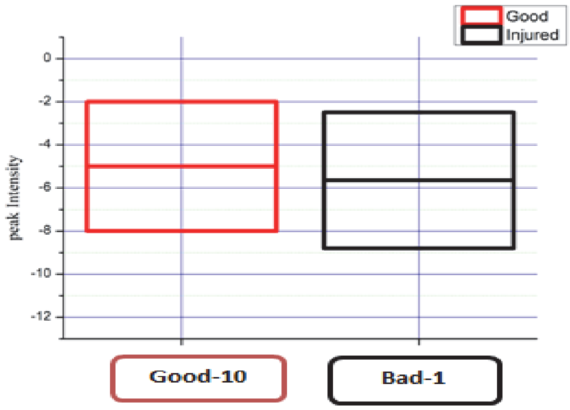

Figure 5 Boxplot of intensity of 10 good and 1 injured individual

5 CONCLUSION

A modern body wearable sensor system has been defined, which can automatically segment the different activities. It classifies them through unregulated conditions outside, extracts acceleration of the high impact and measures the knee and hip joint angles of extension-flexion, which adopt continuous data processing to generate all reliable and comparable data to this normative method. In conjunction with a DFET function extraction methodology, the proposed new method employed an algorithm for DFET- random forest testing to effectively identify training events with up to 93% overall precision. The position of each sensor, as well as its corresponding body section direction, has been determined. Thus, the extension and flexion of knee bone and hip bone angles have been obtained via the wearable sensors on the thighs and shanks of the DGD-based device. A data review method at the end of the pipelines for an objective measurement of the movement methodology has been given with measured knee and hip joint angles and effect accelerations. In analyzing the continuous joint angle results, the trials must be reported before the averages are produced to ensure that both the community results and person dependent data are retained. To improve the exoskeleton's human-machine coordination efficiency, continuous joint angle estimation based on the surface electromyography signal can be used. The joint angle is simple to calculate. The constant joint angle estimate will contribute to smooth exoskeleton control and thus has wide potential for use. If guaranteed, the system proposed has a significant ability to control athletes during preparation and competition to recognize the deciding variables correlated with injury and results, which recognize individuals early in the track before severe tissue damage, and assess individuals. They are predisposed to injury through activity practices.

Acknowledgments

This research was funded by the Shijiazhuang Higher Education Science Research Project - Empirical Study on the Impact of Blended Teaching on Vocational Aerobics Courses, Project Number: 20230387.

6 REFERENCES

[1] Weerapong, P., Hume, P. A., & Kolt, G. S. (2012). The mechanisms of massage and effects on performance, muscle recovery and injury prevention. *Sports medicine*, *35*(3), 235-256(2005). https://doi.org/10.2165/00007256-200535030-00004

[2] Hicks, A. L., Martin, K. A., Ditor, D. S., Latimer, A. E., Craven, C., Bugaresti, J., & McCartney, N. (2003). Long-term exercise training in persons with spinal cord injury: effects on strength, arm ergometry performance and psychological well-being. *Spinal cord*, *41*(1), 34-43. https://doi.org/10.1038/sj.sc.3101389

[3] Hammer, W. I. (2008). The effect of mechanical load on degenerated soft tissue. *Journal of Bodywork and Movement Therapies*, *12*(3), 246-256. https://doi.org/10.1016/j.jbmt.2008.03.007

[4] Henao-Murillo, L., Ito, K., & van Donkelaar, C. C. (2018). Collagen damage location in articular cartilage differs if damage is caused by excessive loading magnitude or rate. *Annals of biomedical engineering*, *46*(4), 605-15. https://doi.org/10.1007/s10439-018-1986-x

[5] Smale, K. (2018). *Relating subjective and objective knee function after anterior cruciate ligament injury through biomechanical and neuromusculoskeletal modelling approaches*. University of Ottawa.

[6] Lorenzetti, S. (2016). Strength training: Towards subject specific modelling, individual internal loading conditions and design of exercises. *research-collection.ethz.ch* https://doi.org/10.3929/ethz-a-010817889

[7] James, O., Jilke, S.R., & Van Ryzin, G. G. (2017). *Experiments in public management research: Challenges and contributions*. Cambridge University Press. https://doi.org/10.1017/9781316676912

[8] Drezner, J. A., O'Connor, F. G., Harmon, K. G., Fields, K. B., Asplund, C. A., Asif, I. M., Price, D. E., Dimeff, R. J., Bernhardt, D. T., & Roberts, W. O. (2018). AMSSM position statement on cardiovascular preparticipation screening in athletes: current evidence, knowledge gaps, recommendations and future directions. *British Journal of Sports*, *51*(3), 153-67. https://doi.org/10.1136/bjsports-2016-096781corr1

[9] Camomilla, V., Bergamini, E., Fantozzi, S., & Vannozzi, G. (2018). Trends supporting the in-field use of wearable inertial sensors for sport performance evaluation: A systematic review. *Sensors*, *18*(3), 873. https://doi.org/10.3390/s18030873

[10] Ancillao, A., Tedesco, S., Barton, J., & O'Flynn, B. (2018). Indirect measurement of ground reaction forces and moments by means of wearable inertial sensors: A systematic review. *Sensors*, *18*(8), 2564. https://doi.org/10.3390/s18082564

[11] Nedergaard, N. J. (2017). *Whole-body biomechanical load monitoring from accelerometry in team sports. Doctoral dissertation, Liverpool John Moores University.*

[12] El-Sheimy, N. & Youssef, A. (2020). Inertial sensors technologies for navigation applications: state of the art and future trends. *Satellite Navigation*, *1*(1), 2. https://doi.org/10.1186/s43020-019-0001-5

[13] Colyer, S. L., Evans, M., Cosker, D. P., & Salo, A. I. (2018). A review of the evolution of vision-based motion analysis and the integration of advanced computer vision methods towards developing a markerless system. *Sports medicine-open*, *4*(1), 24. https://doi.org/10.1186/s40798-018-0139-y

[14] Teague, C. N., Hersek, S., Töreyin, H., Millard-Stafford, M. L., Jones, M. L., Kogler, G. F., Sawka, M. N., & Inan, O. T. (2016). Novel methods for sensing acoustical emissions from the knee for wearable joint health assessment. *IEEE Transactions on Biomedical Engineering*, *63*(8), 1581-90. https://doi.org/10.1109/tbme.2016.2543226

[15] Seshadri, D. R., Li, R. T., Voos, J. E., Rowbottom, J. R., Alfes, C. M., Zorman, C. A., & Drummond, C. K. (2019). Wearable sensors for monitoring the internal and external workload of the athlete. *NPJ digital medicine*, *2*(1), 1-8. https://doi.org/10.1038/s41746-019-0149-2

[16] Kamišalić, A., Fister, I., Turkanović, M., & Karakatič, S. (2018). Sensors and functionalities of non-invasive wrist-wearable devices: A review. *Sensors*, *18*(6), 1714. https://doi.org/10.3390/s18061714

[17] Kutilek, P., Volf, P., Viteckova, S., Smrcka, P., Lhotska, L., Hána, K., Krivanek, V., Doskocil, R., Navrátil, L., Hon, Z., & Stefek, A. (2017). Wearable Systems and Methods for Monitoring Psychological and Physical Condition of Soldiers. *Advances in Military Technology*, *12*(2). https://doi.org/10.3849/aimt.01186

[18] Howard, R. M. (2017). The application of data analysis methods for surface electromyography in shot putting and sprinting. https://doi.org/10.13140/RG.2.2.15907.04640

[19] Mombaur, K., Vallery, H., Hu, Y., Buchli, J., Bhounsule, P., Boaventura, T., Wensing, P. M., Revzen, S., Ames, A. D., Poulakakis, I., & Ijspeert, A. (2017). Control of Motion and Compliance. *Bioinspired Legged Locomotion*, 135-346. https://doi.org/10.1016/b978-0-12-803766-9.00006-3

[20] Yang, M., Gao, C., & Han, J. (2022). Edge Computing Deployment Algorithm and Sports Training Data Mining Based on Software Defined Network. *Computational Intelligence and Neuroscience*, *2022*(1), 1-11. https://doi.org/10.1155/2022/8056360

[21] de Barbaro, K. (2019). Automated sensing of daily activity: A new lens into development. *Developmental psychobiology*, *61*(3), 444-64. https://doi.org/10.1002/dev.21831

[22] Lonsdorf, T. B., Menz, M. M., Andreatta, M., Fullana, M. A., Golkar, A., Haaker, J., Heitland, I., Hermann, A., Kuhn, M., Kruse, O., & Drexler, S. M. (2017). Don't fear "fear conditioning": Methodological considerations for the design and analysis of studies on human fear acquisition, extinction, and return of fear. *Neuroscience & Biobehavioral Reviews*, *77*, 247-85. https://doi.org/10.1016/j.neubiorev.2017.02.026

[23] Prakash, C., Kumar, R., & Mittal, N. (2018). Recent developments in human gait research: parameters, approaches, applications, machine learning techniques, datasets and challenges. *Artificial Intelligence Review*, *49*(1), 1-40. https://doi.org/10.1007/s10462-016-9514-6

[24] Poulos, C. C. (2019). *Exploring the Relationship between Performance on a Series of Squat based Movement Tasks and Passive Range of Motion Capacity - Is Successful Performance a Valid Method of Ruling out Range of Motion Restrictions?* Doctoral dissertation.

Contact information:

Baolei ZHANG
Nanfang College Guangzhou,
Guangzhou, 510900, China

Juan YANG
Shijiazhuang Preschool Teachers College,
Shijiazhuang, 050228, China

Yan PENG
North University of China,
Taiyuan, 030500, China

Chong LIU
(Corresponding author)
Physical Education College,
Chizhou University,
Anhui, 247000, China
E-mail: dugucanbao2006@126.com